AIMS Materials Science, 9(2): 214–235.
DOI: 10.3934/matersci.2022013
Received: 26 September 2021
Revised: 10 January 2022
Accepted: 17 January 2022
Published: 17 February 2022

http://www.aimspress.com/journal/Materials

Research article

Enhanced structural, thermal, mechanical and electrical properties of nano ZTA/epoxy composites

Chaitra Srikanth[1], G.M. Madhu[1,2,*] and Shreyas J. Kashyap[1,2]

[1] Department of Chemical Engineering, M S Ramaiah Institute of Technology, MSR Nagar, Bangalore, Karnataka, 560054, India
[2] Centre for Advanced Materials Technology, M S Ramaiah Institute of Technology, MSR Nagar, Bangalore, Karnataka, 560054, India

* **Correspondence:** Email: gmmadhu@gmail.com; Tel: +91-9845381349, Fax: +91-080-23603124.

Abstract: Epoxy composites were prepared by doping nano Zirconia Toughened Alumina (ZTA) which were synthesized by solution combustion method into epoxy resin and hardener. Initially ZTA nanopowder was characterized to check its purity, morphology and to confirm its metal-oxide bonding using XRD, SEM and FTIR respectively. The thermal properties such as TGA and DTG were also analysed. The polymer composites were obtained by uniformly dispersing ZTA nanopowder into epoxy using an ultrasonicator. Polymer composites of various concentrations viz, 0.5, 1, 1.5, 2 and 2.5 wt% were synthesized, all concentrations were prepared on weight basis. All the polymer composites were tested for compression properties, flexural properties and tensile properties. Best results for all the mechanical properties were obtained for epoxy with 1.5 wt% ZTA composites. Electrical properties such as breakdown voltage and breakdown strength were analysed and outstanding results were observed for epoxy with 2.5 wt% ZTA composite.

Keywords: ZTA; epoxy; SEM; UV-Vis Spectra; Raman Spectra; TGA; DTG; compressive properties; flexural properties; breakdown voltage

1. Introduction

High performance engineering polymers are extensively used for mechanical applications due to their good modulus values, strength, toughness, low creep, high wear resistance, flexural and

compressive strength. They also offer good resistance towards thermal and chemical degradation [1,2]. Generally thermosetting polymers such as epoxies are preferred for these applications. Epoxies offer some undesirable qualities as they tend to be brittle due to the high degree of crosslinking between the polymeric chains. This may yield a detrimental effect on resistance against impact, wear mechanism, structural ability and performance of engineering materials [1,2]. However, all these undesirable properties in an epoxy can be improved with the addition of inorganic particles. The choice of the reinforcing material and its concentration in the epoxy decides the properties of the entire composite itself. Dimension, distribution, solid phase and interfacial interactions of the nanofiller with epoxy play a vital role in deciding the formation of a new class of composite material [1,2].

Significant information on epoxy/zirconia composites are available. Dorigato et al. [3] synthesized zirconia nanoparticles by sol gel technique and further calcinated the nanopowder. After calcination, they studied the effect of nanofiller content on shear strength and other tensile mechanical properties such as Young's Modulus, tensile strength and strain at break. They found that, all the mechanical tensile properties were enhanced with addition of zirconia as a nanofiller in epoxy [3]. Bondioli et al. [4] synthesized submicron zirconia particles by sol gel method. Two batches were prepared, first batch zirconia particles with average particle size of 220 nm and second batch with average particle size of 550 nm.

Both the batches were doped separately into epoxy and tested for their tensile mechanical properties. The results showed that, enhancement in elastic modulus was observed in both the cases as compared to neat epoxy. However, best results were observed for the first batch samples with an average particle size of 220 nm [4]. Alumina nanoparticles were reinforced into epoxy matrix and the mechanical properties such as tensile modulus, stress at break and fracture toughness were investigated [5]. The effect of these composites on aluminium single-lap bonded joints were prepared and tested for shear strength and fatigue life of the bonded joints. The results showed that the alumina based epoxy composites not only exhibited improved mechanical properties, they also enhanced the static and fatigue resistance of single-lap aluminium joints under shear conditions [5]. Yu et al. [6] synthesized alumina nanoparticles and modified it by using γ-aminopropyl triethoxysilane to react with the hydroxyl groups and compared the results of mechanical properties. The results showed that, modified alumina particles exhibited better flexural properties for 3 wt% loading of alumina in epoxy. The flexural strength and flexural modulus were enhanced by 55% and 77.1% respectively [6].

Zirconia toughened Alumina (ZTA) is an advanced ceramic material due to its high hardness, strength, corrosion resistance, good thermal shock resistance, excellent insulating materials, high wear resistance and high compressive strength under elevated temperatures [7–9]. This makes it a promising material of interest for various applications such as cutting tools, biomedical implants, structural parts, pump pistons, spraying nozzles, biomaterials for hip arthroplasty and dental applications [7–9]. From the above cited literatures, it is evident that, research work on zirconia/epoxy composites as well as alumina/epoxy composites are available, whereas research work on ZTA/epoxy composites remains unexplored. Enhanced mechanical properties such as tensile, compression and flexural properties of ZTA/epoxy composites has been presented for the first time.

In the present study, ZTA nanoparticles are synthesized by solution combustion method. The synthesized nanoparticles were characterized for their morphology using SEM, the crystallinity and

phases of the nanoparticle was characterized using XRD. The metal oxide bonding in the nanomaterial was confirmed using FTIR spectra. The ZTA nanoparticles were further doped into a Bisphenol-A based epoxy resin along with a hardener. The doping concentration was from 0–2.5 wt% of ZTA nanoparticles into epoxy. To maintain homogeneity and uniform mixing between the epoxy and the nano filler, the mixture was ultrasonicated using an ultrasonicator. The optical properties of ZTA/epoxy composites were analysed using UV-Vis Spectra and Raman spectra. All the mechanical properties were tested using Zwick Universal Testing Machine (UTM). The effect of doping concentration on the mechanical properties such as tensile properties, compression properties and flexural properties of the epoxy composites were investigated and reported. The electrical properties such as breakdown voltage and strength are also reported. These high performance polymers may find extensive use in coatings, aerospace industry, biomedical and high voltage insulation applications.

2. Materials and methods

2.1. Chemicals

Zirconyl nitrate was obtained from M/S Loba Chemie laboratory reagents and fine chemicals. Molecular weight and purity for zirconyl nitrate were 231.23 g/mol and 99.5% respectively. Aluminium nitrate nonahydrate was procured from M/s Merck specialities private limited. Molecular weight and purity for zirconyl nitate were 375.13 g/mol and 98.5% respectively. Urea was obtained from S D Fine-Chem limited having a molecular weight of 60.06 g/mol. Lapox L-12, a Bisphenol-A based resin epoxy resin was used for our experimental study, along with a polyamine K-6 hardener which was used as a curing agent. Urea was used as a fuel for the solution combustion reaction. Double distilled water was used for dissolving zirconyl nitrate, aluminium nitrate nonhydrate and urea.

2.2. Synthesis of ZTA nanoparticles

ZTA nanopowder was synthesized by solution combustion method [10]. Stoichiometric quantities of zirconyl nitrate, aluminum nitrate nonhydrate and urea were mixed and dissolved in double distilled water. The reaction was allowed to take place in a preheated muffle furnace set at 600 ℃ for 45 min. Self-ignition of the reaction mixture took place, resulting in the formation of white, foamy compound. This was later crushed softly to yield a white, soft porous ZTA nanopowder which was later calcinated in a muffle furnace for 600 ℃ for one hour.

2.3. Fabrication of ZTA nano-filler in epoxy

A known quantity of epoxy was taken and sonicated for 40minutes in an ultrasonicator (200 W), the temperature of the epoxy began to rise to 60–70 ℃. To prevent further heating, the epoxy was allowed to cool to room temperature and later it was mixed with the hardener. The mixture was allowed to dry at room temperature for 48 h. A standard stoichiometric quantity of 90% epoxy resin and 10% hardener composition was maintained to prepare all the samples. Once the epoxy resin and hardener mixture was cooled to room temperature, it was casted on a rectangular mould. The

reaction mixture was allowed to dry for 2–3 d. ZTA based epoxy composites were prepared by a similar procedure. Stoichiometric quantities of nanofiller was calculated on weight basis such as 0.5 wt%, 1 wt%, 1.5 wt%, 2 wt% and 2.5 wt%. Epoxy resin and nanofiller of known quantity were taken and mixed using an ultrasonicator for 40 min. The mixture was later cooled to room temperature followed by addition of hardener and further mixing and casting on the rectangular mould. Care was taken to avoid bubble formation during casting procedure. Thickness of plain epoxy was found to be 2.6 mm, whereas for epoxy composites it was found to be ranging from 2.62 to 2.79 mm. Thickness measurements were made using LCD digital Vernier callipers (Make: Mitutoyo).

2.4. Characterization techniques and measurements

Preliminary characterization of the nanofiller for its structural and morphology features is very much essential, as it plays a vital role in deciding the properties of the polymer composites. The surface morphology of nano powders and the tensile fractured surface of the polymer composites were investigated using a Field Emission Scanning Electron Microscope (FESEM) from Zeiss (Gemini ultra55) keeping an accelerating voltage of 5 kV. The instrument was also coupled to an EDS detector (Oxford INCA EDS detector) for Energy Dispersive X-ray spectroscopy (EDX). Prior to each measurement, the samples were Au-sputter coated. Fourier Transform Infrared Spectrometer in transmittance mode was used to analyse our nanopowder in the spectral range of 4000–400 cm^{-1} at a resolution of 4 cm^{-1}. The samples were also characterised for optical properties such as UV-Vis spectra and Raman spectra, and the same is reported in detail in Supplementary Information section. Thermal stability was analysed by NETZSCH 449 F1 Jupiter simultaneous thermal analyser (STA) in the temperature range of 40–800 ℃ with a ramp rate of 10 ℃/min under dry N_2 atmosphere. X-ray diffraction analysis (XRD) of was performed on a D8 Advance X-ray diffractometer with Cu kα radiation (λ = 1.54 Å) operated at 40 kV and 40 mA. Diffraction patterns of the samples were collected by scanning over the 2θ angular range of 10–80° with a step of 0.02°. Bruker Alpha FTIR spectrometer was used to analyse the samples in transmittance mode in the spectral range of 4000–500 cm^{-1} with a resolution of 4 cm^{-1}. Zwick Universal Testing Machine (UTM) was used to test all the mechanical properties such as Tensile, compressive and flexural properties of the epoxy based polymer composites. ASTM D638 standard testing procedure was used to perform tensile properties testing with a crosshead speed of 10 mm/min. ASTM D695 standard testing procedure was used to perform compression properties testing with a testing speed of 2 mm/min. ASTM D790 standard testing procedure was used to perform flexural properties testing with a preload speed of 5 mm/min. Breakdown voltage was measured using experimental set up as per ASTM D3756-97. Three samples for each composition of the composite was taken and tested. The average values are reported.

3. Results and discussions

3.1. Scanning Electron Microscopy (SEM) and Energy Dispersive X-ray Analysis (EDX)

Figure 1 shows the SEM/EDX results of the as-synthesised ZTA nanoparticles. The morphology seems to have micro-pores in addition to a rough and irregular surface. The micrograph

also shows a minute crack which was probably originated during high temperature calcination [11]. EDX spectrum (Figure 1b) shows three main peaks at ~0.3 keV, 1.5 keV and 2.2 keV belonging to elements O, Al and Zr respectively. The elemental composition in atomic % for oxygen, aluminium and zirconium were found to be 72.34, 22.88 and 4.79 respectively.

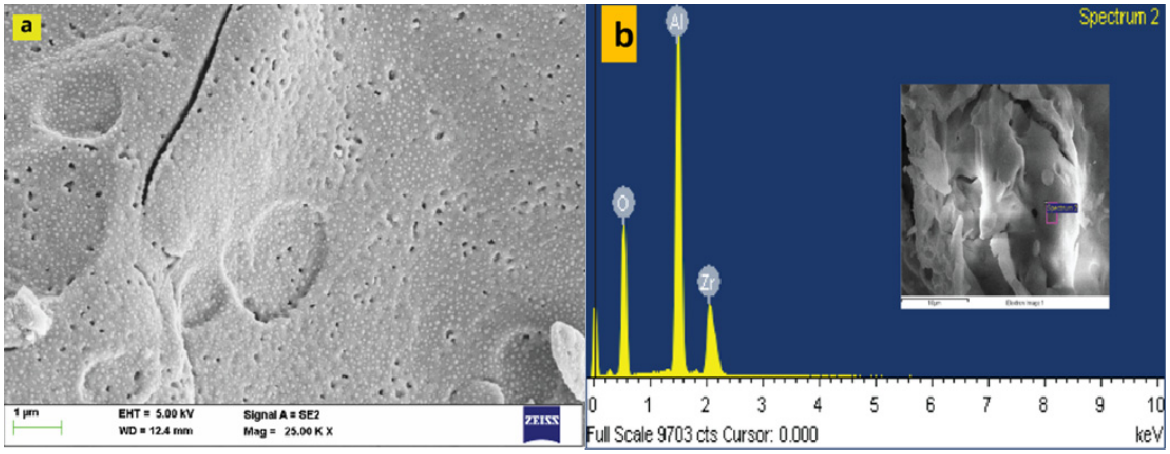

Figure 1. (a) SEM image of ZTA nanopowder calcined at 600 °C and (b) EDX spectrum of the ZTA. Inset in (b) shows the scan area for EDX.

3.2. X-ray Diffractometer (XRD)

Powder XRD was used to analyse and characterize ZTA nanopowder for its crystallinity, phases and lattice parameters. As evident from Figure 2a, the sharp peaks indicate that ZTA nanopowder synthesized by solution combustion method is a crystalline material. Zirconia and alumina were found to be existing in tetragonal and α-alumina phase respectively, the same has been confirmed using Raman Spectroscopy (Figure S1 Supplementary Information section). The Raman spectroscopy of ZTA nanopowder showed highly prominent zirconia peaks existing in tetragonal phase and lesser prominent peaks of alumina existing in alpha phase. Zirconia diffraction peaks were obtained at 2θ = 30.25°, 34.60°, 35.31°, 50.27°, 50.80°, 59.34°, 60.28° and 62.93° with corresponding lattice planes (101), (002), (110), (112), (200), (103), (211) and (202) respectively. α-alumina diffraction peaks were obtained at 2θ = 25.57°, 37.76°, 46.16°, 57.48°, 59.72°, 66.49°, 68.18°, with corresponding lattice planes (012), (110), (202), (024), (116), (214) and (300) respectively. A characteristic peak splitting phenomena was observed at 50.15° and 50.70° which was a strong evidence to show that zirconia existed in tetragonal phase. The diffraction peak positions of ZrO_2 and Al_2O_3 matched with ICDD No. 01-079-1766 and ICDD No. 00-010-0173 respectively. All the diffraction peak positions obtained for ZTA were matching to that obtained by various researchers [10,12,13]. Average crystal size was calculated using Debye–Scherrer formula. The smallest size and the largest size of the crystal were found to be 24.22 nm and 54.34 nm.

Figure 2b reveals the XRD data of plain epoxy and nano ZTA/epoxy composites. Since epoxy is an amorphous polymer [14], its XRD image does not reflect any sharp peaks. The prominent peak observed at 2θ = 20° among all the epoxy samples indicates epoxy peak [15]. Addition of ZTA nanoparticles into epoxy showed increase in crystalline peaks in the epoxy composites. The sharp crystalline peaks of ZTA molecules became very prominent for epoxy with 2.5 wt% ZTA, which

closely matched the peak positions obtained for ZTA nanopowder. Another interesting phenomenon that was observed for epoxy with 2.5 wt% ZTA was, it further broadened the epoxy peak and made it look less dominant compared to the plain epoxy peak. Similar results were observed for enhancement in Raman intensity and it was found to be the highest for epoxy with 2.5 wt% ZTA as indicated in Figure S2 in Supplementary Information section.

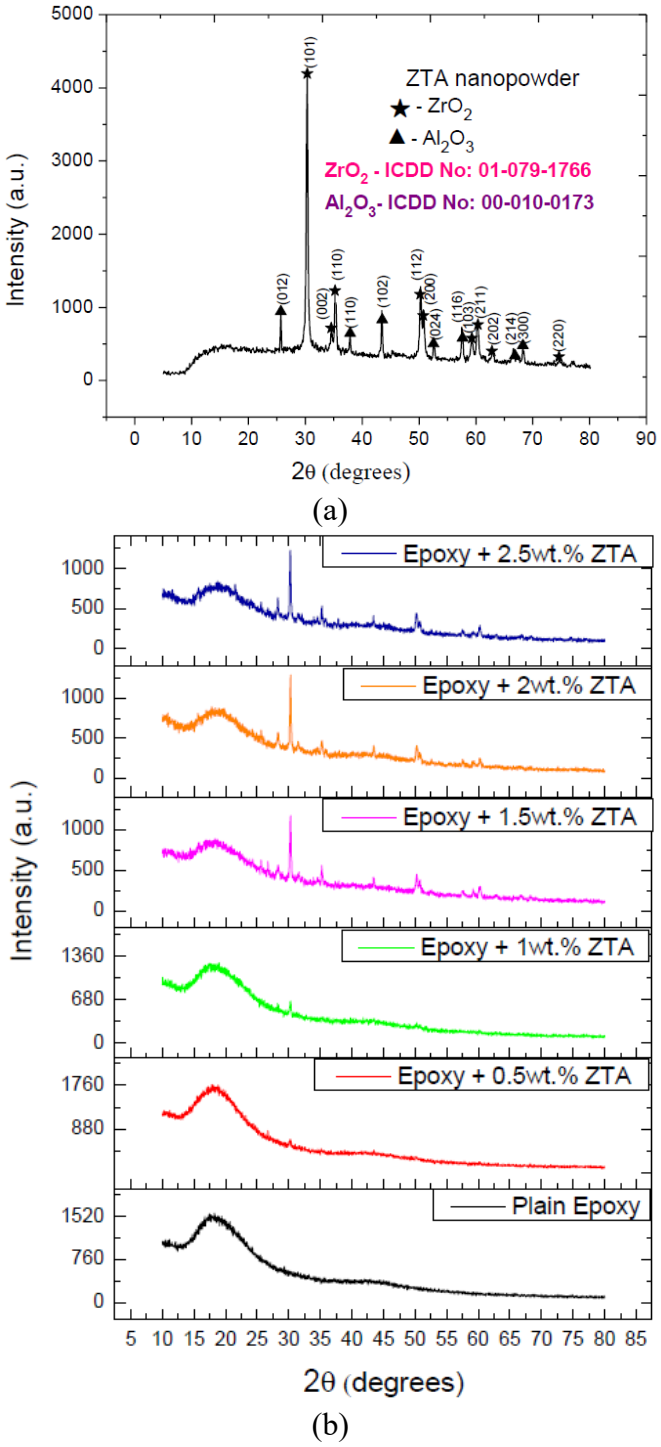

Figure 2. (a) XRD image of ZTA nanopowder, (b) XRD image of plain epoxy and nano ZTA/epoxy composites.

3.3. Thermogravimetric Analysis (TGA) and Derivative Thermo-Gravimetry (DTG)

TGA and DTG curves for epoxy composites are represented in Figure 3a,b respectively. Parameters required for its evaluation are presented in Table 1. In Table 1, $T_{10\%}$ denotes the temperature after 10% weight loss, sometimes regarded as the onset of degradation. Further, $T_{50\%}$ is the temperature after 50% of weight loss T_{max} denotes the temperature at maximum decomposition, dW/dT corresponds to the weight loss rate at T_{max} and $\%char_{800}$ is the residual weight remaining after completion of the experiment. It can be observed that the incorporation of the nanofiller might have interfered with the cross-linking density of the base matrix resulting in early onset of degradation in a few samples. This trend is not generally observed in amine-cured epoxy composites; however, some researchers have observed such phenomenon [16–20]. The agglomerations of nanoparticles cause spatial obstruction in the matrix leading to increased free volume inside the epoxy polymer. The first step of degradation observed near 150–350 °C is due to the deterioration of low molecular weight substances such as interstitial water, curing or hardening agents and unreacted epoxy chains leading to C–C unsaturation [21,22]. The second large degradation step observed around 400–500 °C is due to the decomposition of long chain aromatic rings. It can be noted that at this stage of the process, the stability of the composites has been significantly enhanced. For instance, $T_{50\%}$ of epoxy with 0.5 wt% ZTA is approximately 48 °C more than that for pristine epoxy (375.89 °C). Nano inclusions can act as a barrier and hinder polymer mass transport across them [23]. In addition, it is observed that the maximum decomposition temperature of epoxy with 0.5 wt% ZTA is approximately 70 °C greater than plain epoxy (T_{max} = 362.84 °C). However, for epoxy with 1.0 wt% ZTA and epoxy with 1.5 wt% ZTA, T_{max} does not seem to have increased significantly. This is due to irregular dispersion of nanoparticles inside the polymer matrix. Controlling the dispersion of nanoparticles in thermoset polymer matrices are crucial in enhancing the overall properties of composites. The $\%char_{800}$ also shows irregular trend due to the same reason. Interestingly, this observation indicates that the incorporation of nanoparticles into the epoxy polymer does not greatly influence its thermal stability.

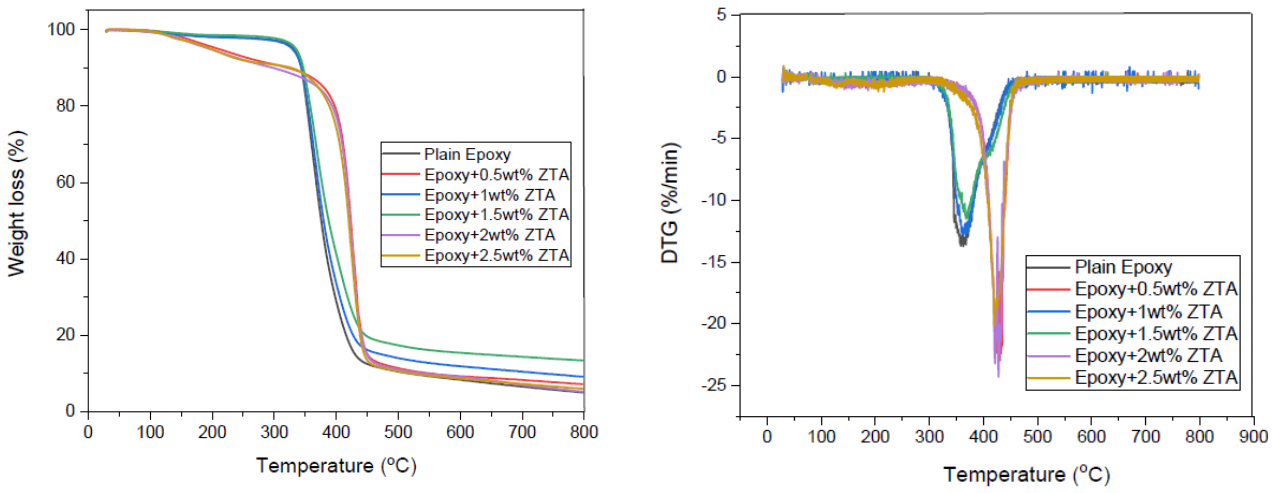

(a) (b)

Figure 3. (a) TGA thermogram of plain epoxy and nano ZTA/epoxy composites, (b) DTG thermograms of plain epoxy and nano ZTA/epoxy composites.

Table 1. Thermal data of plain epoxy and nano ZTA/epoxy composites.

ZTA content	$T_{10\%}$ (°C)	$T_{50\%}$ (°C)	T_{max} (°C)	$(dW/dT)_{max}$	$\%char_{800}$
0.0	375.89	362.84	363.09	−13.70	5.04
0.5	423.66	430.59	428.35	−22.95	7.23
1.0	363.21	363.21	361.01	−12.80	9.18
1.5	367.88	367.88	370.50	−11.48	13.41
2.0	527.29	427.29	427.84	−24.72	5.25
2.5	420.23	420.23	419.76	−20.15	6.02

3.4. Fourier Transform Infrared spectroscopy (FTIR spectra)

The detailed FTIR spectra of calcinated ZTA nanopowder has been shown in Figure 4a. Significant peaks obtained during the analyses are indicated in the range of 400–1100 cm^{-1}. Eleven prominent peaks were obtained at 411 cm^{-1}, 436 cm^{-1}, 482 cm^{-1}, 517 cm^{-1}, 557 cm^{-1}, 584 cm^{-1}, 635 cm^{-1}, 703 cm^{-1}, 759 cm^{-1} and 1051 cm^{-1}. The peak broadening absorption band obtained in the range of 1070–612 cm^{-1} are corresponding to the Al–O vibrations [24,25]. The peak bending absorption band obtained in the range of 400–590 cm^{-1} are the characteristic Zr–O vibrations [25,26]. Hence, the metal-oxide interactions between the molecules are clearly evident. No additional peaks were observed; this indicates the purity of the nanopowder. Peak broadening was observed in UV-Vis spectra of ZTA nanopowder in Figure S3 (Supplementary Information section), this indicates that at low wavelength the sample exhibits high UV-Shielding capacity.

To understand the interaction between the synthesized ZTA nanoparticles and the epoxy, FTIR was performed for each and every polymer composite along with plain epoxy. Figure 4b shows the FTIR spectra of nano ZTA/epoxy composites. The FTIR spectrum of plain epoxy showed a broad peak around 1005 cm^{-1} which is recognised to be epoxide ring vibration [27,28]. An additional peak at 1236–1242 cm^{-1} is also contributed due to epoxide stretching vibration [27,28]. The prominent peak obtained at 787 cm^{-1} indicates the presence of ketone group [29]. The peaks appearing at 1503 cm^{-1} and 1610 cm^{-1} indicate C=C stretching group [28]. The peak at 2954 cm^{-1} indicates symmetrical stretching of CH_3 group [28]. The peaks appearing in the range of 3150–3789 cm^{-1} confirm the presence of hydroxyl group, which are due to the absorbed water molecules or the hydrogen bonded to the ZTA nanoparticles [28]. The peaks appearing at around 625–633 cm^{-1} and 815–822 cm^{-1} indicate the metal oxide interactions and confirm the presence of ZTA molecules [28]. It is clearly evident that, with increase in filler concentration, the peak position at 822 cm^{-1} tends to become sharper and more prominent. Whereas, the peak at 787 cm^{-1} tends to diminish gradually. It is also observed that, broadening of peaks at 2919 cm^{-1} and 3347 cm^{-1} have attributed to hydroxyl stretching groups which are resulted due to the condensation of hydrolysed ZTA nanoparticles in the epoxy matrix [28]. This phenomenon occurs when the hardener is added to the epoxy resin along the filler which eventually result in the crosslinking of the polymer composites. UV-Vis spectra of nano ZTA/epoxy composites also confirmed enhanced interaction of nanofiller with epoxy as shown in Figure S4 (Supplementary Information section) and the results revealed that epoxy loaded with 2.5% ZTA exhibits excellent UV shielding efficiency among all the samples at a very wide wavelength range (200–1100 nm).

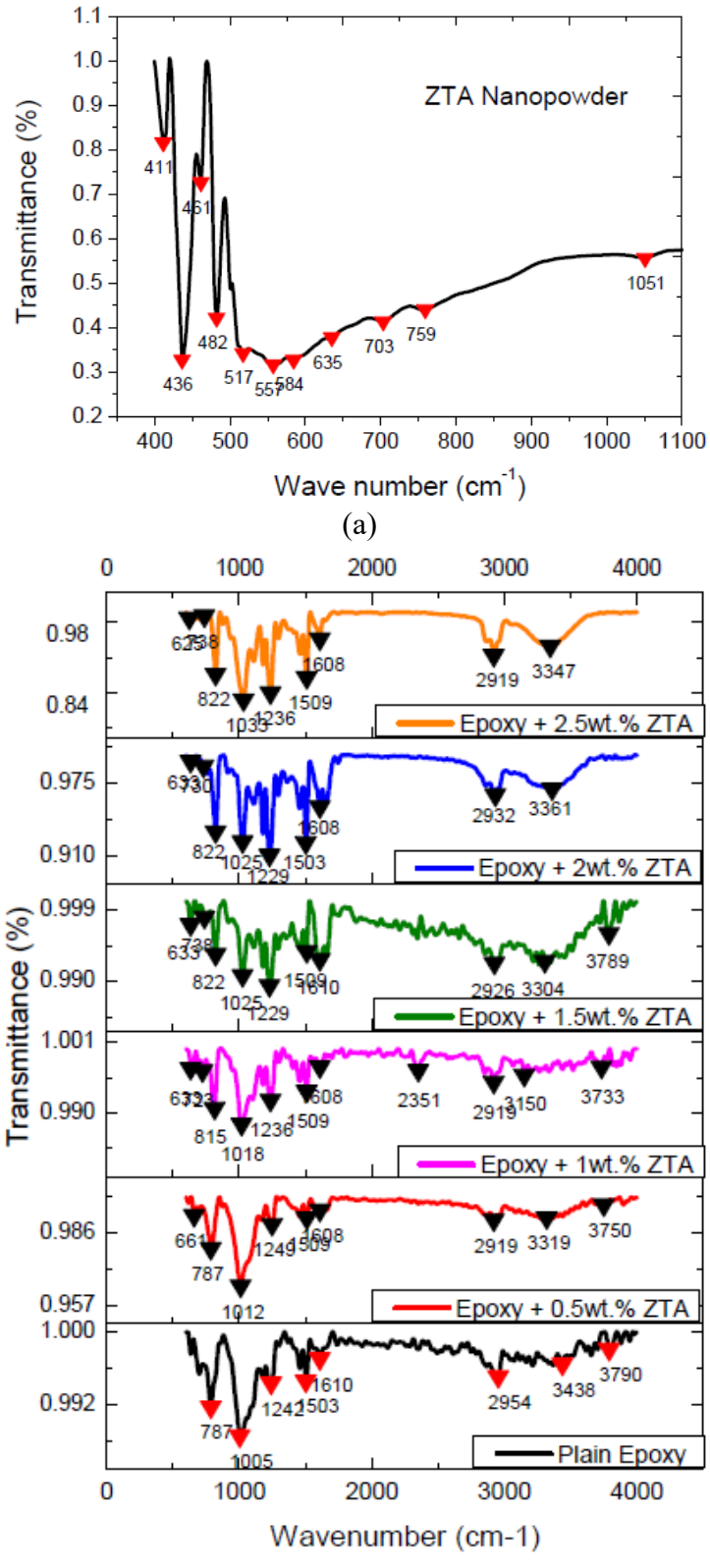

Figure 4. (a) FTIR spectra of ZTA nanopowder, (b) FTIR spectra of plain epoxy and nano ZTA/epoxy composites.

3.5. Mechanical properties

Mechanical properties such as compressive properties, flexural properties and tensile properties were tested for plain epoxy and nano ZTA/epoxy composites. Compressive properties testing was carried out as per ASTM D695, flexural properties were tested as per ASTM D790 and tensile properties were tested as per ASTM D638.

3.6. Compressive properties

Figure 5a shows the compressive stress vs compressive strain for epoxy composites with varying concentrations of ZTA. It is clear from the graph that, best compressive properties were observed for epoxy with 1.5 wt% ZTA such as highest compressive strength, compressive toughness and compressive modulus. These properties may have been attributed due to enhanced bonding of ZTA molecules with epoxy as well as better load bearing capacity at 1.5 wt% concentration in epoxy. Thus enhancing the compressive load bearing of the epoxy composite. However, at very low concentrations such as 0.5 wt% ZTA in epoxy and with highest concentration of 2.5 wt% ZTA in epoxy, the composite fails to bear the compressive loads. At low concentrations, the ZTA nanoparticles are not binding well with the epoxy and hence it is unable to transfer any loads. Whereas, at very high concentrations, the nanoparticles form agglomerated molecules resulting in crack propagation and fracture mechanism to occur, even at low compressive loads.

Area under the compressive stress vs compressive strain curve gives the compressive toughness of the epoxy composite. Figure 5b shows the effect of ZTA concentration on compressive toughness of the epoxy composites. Initially, compressive toughness was found to decrease with increase in concentration, and reached a maximum at 1.5 wt% concentration of ZTA in epoxy indicating a profound increase of 56.23% as compared to plain epoxy. Further increase in filler loading did not contribute to any increase in the compressive toughness of the epoxy composite.

The compressive strength of plain epoxy and nano ZTA/epoxy composites is as shown in Figure 5c. Increase in ZTA concentration in epoxy resulted in an initial decrease in compressive strength, with further increase at 1.5 wt% ZTA in epoxy a drastic increase of 33.43% was observed as compared to plain epoxy. This may be due to effective cross-linking between the epoxy and nano filler molecules in the polymer composite. The sudden decrease in the compressive strength values with further increase of filler loading may be attributed due to agglomeration of molecules in the epoxy, these agglomerates tend to block the reactive sites present in the nanofiller. As the size of the agglomerated molecules keeps on increasing, there are very few reactive sites left in the nanofiller [30]. There may be another possible reason for such a failure to occur. As the ZTA concentration increases, the agglomerates may also form different layers due to poor adhesion between the epoxy and the ZTA molecules. These layers tend to slide over each other upon application of compressive loads [31]. Hence, contributing to fracture mechanism at low compressive loads, thereby reducing the compressive strength of the epoxy composite.

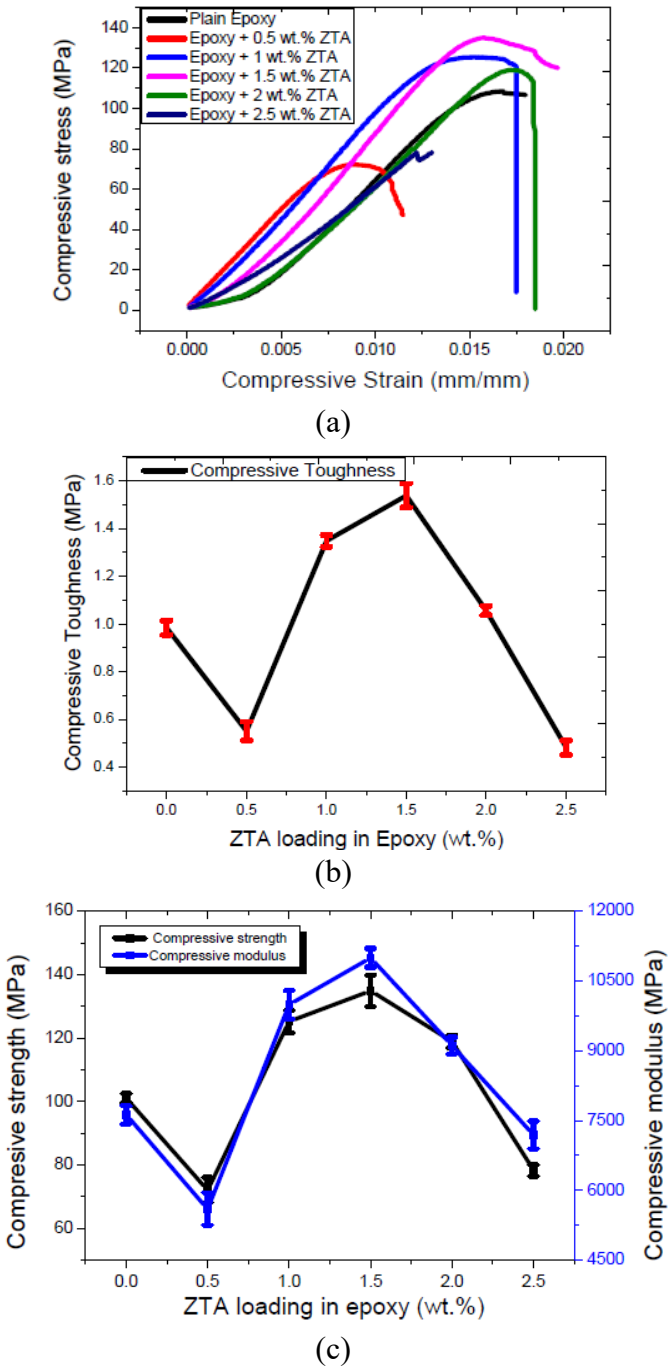

Figure 5. (a) Compressive stress vs compressive strain graph for plain epoxy and nano ZTA/epoxy composites. (b) Compressive toughness of plain epoxy and nano ZTA/epoxy composites. (c) Compressive strength and compressive modulus of plain epoxy and nano ZTA/epoxy composites.

Compressive modulus of plain epoxy and nano ZTA/epoxy composites are as shown in Figure 5c. The compressive modulus value of plain epoxy was found to be 7626 MPa and it increased and reach a maximum of 11000 MPa at 1.5 wt% concentration of ZTA in epoxy. A substantial increase of 44.24% was observed as compared to plain epoxy. Further increase has led to

drastic decrease in the compressive modulus values. This might have occurred due to weakening of interfacial tension existing between the epoxy and nanofiller at high concentrations resulting in formation of localised stresses on application of compressive loads [32].

Compressive properties of plain epoxy and nano ZTA/epoxy composites can be summarized as shown in Table 2. It is evident that at 1.5 wt% concentration of ZTA in epoxy enhanced compressive properties are obtained. All the compressive properties ceases beyond 1.5 wt% concentration of ZTA in epoxy. The reason behind decline of compressive properties with increase in filler content is due to the localised stresses within the polymer composite, formation of ZTA agglomerates contributing to weaker adhesion between matrix and the reinforcement and lastly poor interfacial tension within the polymer composite.

Table 2. Compressive properties of plain epoxy and nano ZTA/epoxy composites.

ZTA content (wt%)	Compressive modulus (MPa)	Compressive toughness (MPa)	Compressive strength (MPa)
0.0*	7626.00	0.98	101.30
0.5	5600.00	0.55	72.10
1.0	9990.60	1.34	125.20
1.5	11000.00	1.53	134.90
2.0	9110.80	1.05	119.00
2.5	7190.00	0.48	78.30

*refers to plain epoxy.

3.7. Flexural properties

The flexural stress vs flexural strain graph for plain epoxy and nano ZTA/epoxy composites are as shown in Figure 6a. It is observed from the figure that flexural strain as well as flexural stress is the highest for epoxy loaded with 1.5 wt% ZTA the values were found to be 0.0205 and 3.22 MPa respectively. The area under the curve was also observed to be the highest for 1.5 wt% concentration of ZTA in epoxy. The flexural stress and flexural strain began to decline with further addition of ZTA in epoxy. Other flexural properties such as flexural strength and flexural modulus also reduced with increase in ZTA concentration beyond 1.5 wt% in epoxy.

Figure 6b shows the flexural strength and flexural modulus of plain epoxy and nano ZTA/epoxy composites. The flexural strength was found to increase with filler content and reached a maximum at 1.5 wt% concentration of ZTA in epoxy. The increase in flexural strength was found to be 60.86% as compared to plain epoxy. The flexural modulus also increased with increase in filler content. The highest flexural modulus was observed to be for 1.5 wt% ZTA in epoxy with a value of 263.8 MPa. the percentage increase in flexural modulus was found to be 71.41% as compared to plain epoxy. This profound increase in flexural strength and flexural modulus values is due to the enhanced and optimised interaction of the ZTA molecules with epoxy. The strong adhesion bonding between the matrix and the filler has contributed to enhanced interfacial interactions resulting into a polymer composite with enhanced load bearing capacity.

The flexural load vs flexural displacement graph for plain epoxy and nano ZTA/epoxy composites is as shown in Figure 6c. It is evident that for a given flexural load, epoxy with 1.5 wt% concentration ZTA exhibits higher flexural displacement than plain epoxy. This means that epoxy

with 1.5 wt% ZTA can withstand higher flexural loads as compared to plain epoxy. The highest load bearing capacity and displacement for plain epoxy were found to be 121.6 N and 1.43 mm/mm respectively. Whereas, highest load bearing capacity and displacement for epoxy loaded with 1.5 wt% ZTA is 125.3 N and 2.34 mm/mm respectively. Another important mechanical property called flexural toughness can be obtained from the area under the curve of flexural load vs flexural displacement graph [33].

Flexural toughness for plain epoxy and nano ZTA/epoxy composites was found using area under the curve of flexural load vs flexural displacement and as shown in Figure 6d. Initially the flexural toughness was found to decrease with increase in filler loading into epoxy. This may be probably due to the poor interaction between the matrix and the reinforcement leading to the failure of the polymer composites at low loads leading to a deflection to occur even at lower loads. Hence, such polymer composites tend to exhibit crack formation, ultimately resulting in fracture mechanism. Incorporation of 1.5 wt% ZTA into epoxy has resulted in a profound increase as well as the highest flexural toughness value. This probably due to the excellent adhesion bonding and enhanced interfacial interaction between epoxy and ZTA nanoparticles. Hence, enhancing the load bearing capacity of the polymer composite.

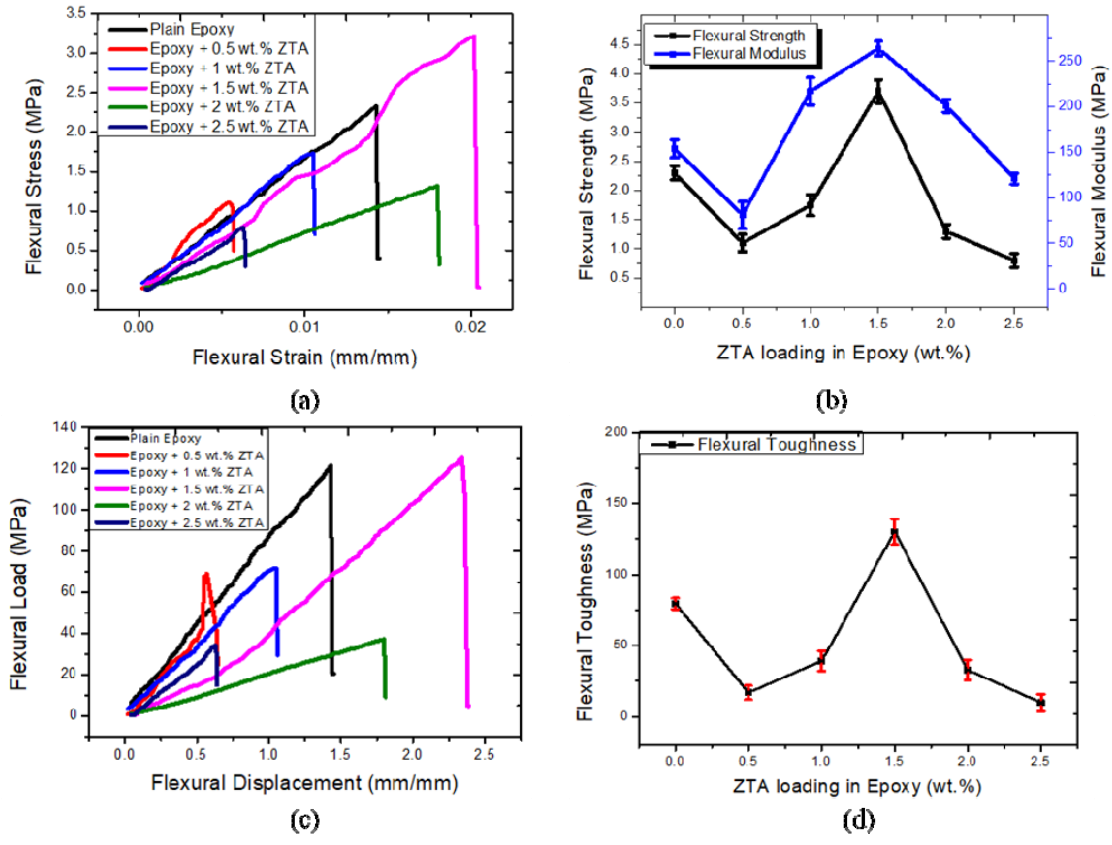

Figure 6. (a) Flexural stress vs flexural strain graph for plain epoxy and nano ZTA/epoxy composites; (b) Flexural strength and flexural modulus of plain epoxy and nano ZTA/epoxy composites; (c) Flexural load vs flexural displacement graph for plain epoxy and nano ZTA/epoxy composites; (d) Flexural toughness of plain epoxy and nano ZTA/epoxy composites.

The flexural properties of plain epoxy and nano ZTA/epoxy composites are summarised in Table 3. The results show that, initially the flexural properties tend to decrease with increase in filler content. Enhanced flexural properties are observed only for epoxy loaded with 1.5 wt% ZTA molecules. High concentration of ZTA nanoparticles in epoxy results in decrease in flexural properties due to the increase in hardness and brittleness of the polymer composite.

Table 3. Flexural properties of plain epoxy and nano ZTA/epoxy composites.

ZTA content (wt%)	Flexural Modulus (MPa)	Flexural Toughness (MPa)	Flexural Strength (MPa)
0.0*	153.90	79.43	2.30
0.5	81.10	16.87	1.10
1.0	217.00	39.18	1.75
1.5	263.80	130.10	3.70
2.0	201.00	32.80	1.30
2.5	121.00	9.74	0.80

*refers to plain epoxy.

3.8. Tensile properties

Figure 7a illustrates the tensile stress vs tensile strain relationship between the epoxy composites. It is evident from the figure that, there is a drastic decrease in the tensile properties of all the polymer composites as compared to plain epoxy. There are two possible reasons for such a phenomenon to occur. Firstly, whenever ZTA is reinforced into a polymer matrix it is liable to increase the hardness of the polymer composite. Increase in hardness has contributed to enhanced brittleness and stiffness of the polymer composite and hence found to be detrimental on the tensile properties [8]. Secondly, the size of zirconia particles plays a vital role in deciding the crack propagation of the polymer composite. When the size of ZTA nanoparticles increase from nanometer level to submicron level, the level of agglomeration also increases, making way for crack nucleation sites. These crack nucleation sites have found to be having a detrimental effect on the tensile properties of the epoxy composites [3].

Tensile toughness of the polymer composites was calculated by finding out the area under the curve of the tensile stress vs tensile strain graph. Figure 7b shows a decline in tensile toughness value with increase in ZTA loading for all the polymer composites. This is due to the fact that the stability of tetragonal zirconia has an impact on tensile toughness of the polymer composites. When zirconia is present in a stable tetragonal phase it reduces the fracture toughness of the epoxy composite. Thus, increase in ZTA content in the epoxy has directly contributed to the decrease in tensile toughness values [30].

Figure 7c depicts the ultimate tensile strength of plain epoxy and nano ZTA/epoxy composites. The ultimate tensile strength is found to decrease with increase in filler loading. This is probably due to stiffness contributed by the inorganic nanofiller which has led to a chain blocking mechanism in the polymeric units resulting in detrimental effects on the ultimate tensile strength of the polymer composite. Decrease in ultimate tensile strength values were found in few literatures where they have incorporated zirconia in epoxy [3] and alumina in epoxy [5] and the tensile properties were studied.

The effect of filler loading on Young's modulus is as shown in Figure 7d Increase in Young's modulus values were observed up to a filler content of 1.5 wt% loading of ZTA in epoxy composites

(83.2% as compared to plain epoxy). Whereas, 27.75% and 25% increase in modulus values were observed in few literatures when epoxy was loaded with 1.5 vol% zirconia nanoparticles and 1.5 vol% alumina nanoparticles in epoxy respectively [3,5]. This shows that ZTA nanoparticles have a better effect on improving epoxy's modulus values as compared to individual nanoparticles. Further increase in ZTA loading has led to reduction in modulus values. This is probably because of the agglomeration of the nanoparticles at higher concentration contributing to crack propagation nuclear sites within the polymer composite itself [5].

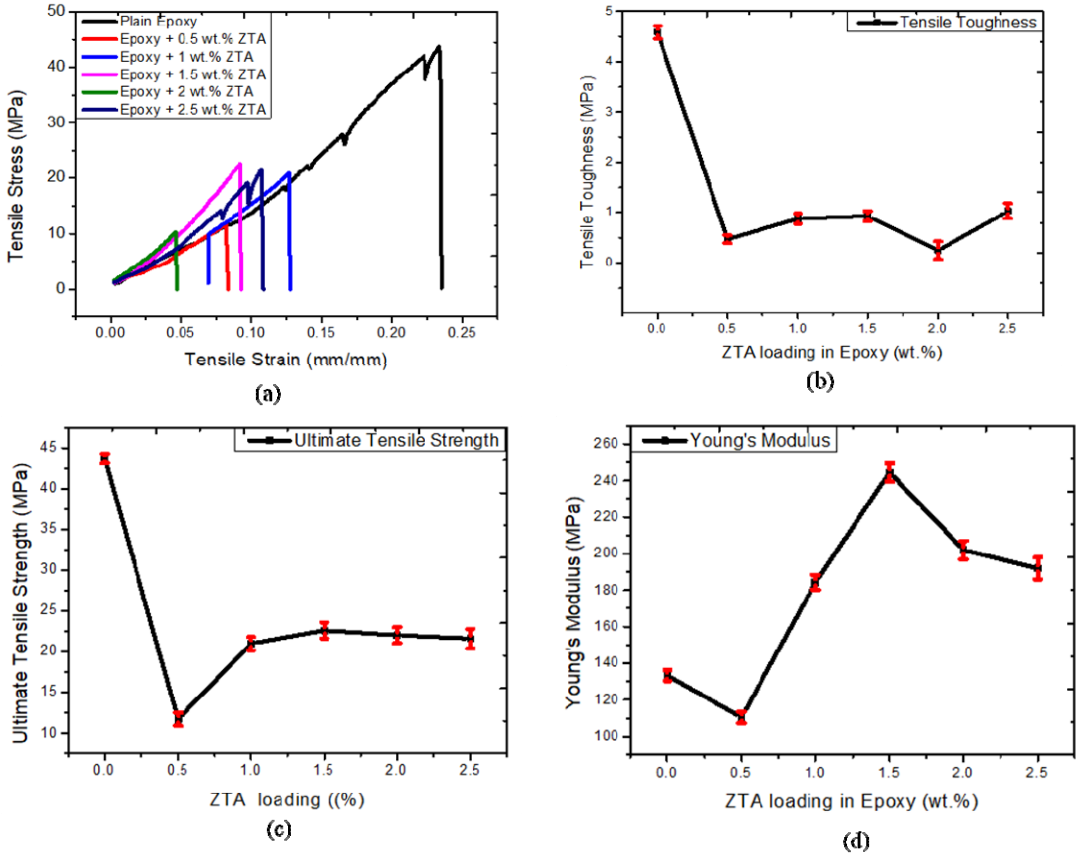

Figure 7. (a) Tensile stress vs Tensile strain graph for plain epoxy and nano ZTA/epoxy composites. (b) Effect of ZTA loading on tensile toughness of epoxy composites. (c) Effect of ZTA loading on ultimate tensile strength of epoxy composites. (d) Effect of ZTA loading on Young's Modulus of epoxy composites.

All the tensile properties of plain epoxy and nano ZTA/epoxy composites are summarized in Table 4. Enhanced Young's modulus values were observed up to 1.5 wt% loading of ZTA molecules due to effective crosslinking between the filler and polymer networks. All the other tensile properties such as tensile toughness, ultimate tensile strength and energy at break-even point are found to reduce with increment in ZTA nanoparticles in epoxy. This shows that stable tetragonal zirconia molecules, agglomerated ZTA molecules have contributed to stiffness and thereby resulting in failure mechanism with filler loadings.

Table 4. Tensile properties of plain epoxy and nano ZTA/epoxy composites.

ZTA content (wt%)	Young's modulus (MPa)	Tensile toughness (MPa)	Energy at break point (N)	Ultimate tensile strength (MPa)
0.0*	133.40	4.58	23.47	43.70
0.5	110.40	0.47	8.170	11.70
1.0	184.30	0.87	12.70	21.00
1.5	244.40	0.92	9.20	22.60
2.0	202.00	0.24	4.60	22.00
2.5	192.00	1.02	10.77	21.60

*refers to plain epoxy.

Tensile fractured SEM images of the fabricated polymer composites are provided in Figure 8a–f. The fractured surface of pure epoxy has a typical smooth surface with several micro-voids and brittle cracks [34]. The nanoparticle-filled epoxy matrix shows similar voids/cavities and irregular humps due to the particle pull-out mechanism (toughening mechanism A) [35]. After tensile fracture, some of the nanoparticles are disintegrated from the base polymer matrix which creates cavities on one side of the fracture and humps from the nano-inclusions on the other side of the fracture. This phenomenon contributes to two toughening mechanisms; one, the voids generated deflect crack propagation (toughening mechanism A) [35–37] and two, the nanoparticle humps resist the path of the crack which ultimately toughens the polymer composite (toughening mechanism C) [36]. The surface is also rough, uneven and contains clusters of nanoparticles. The particle pull-out region can be observed in Figure 8c, where the nanoparticles are seen resisting crack formation by bridging the voids. This phenomenon localizes the stress distribution to some extent. In addition, plastic void growth can be observed from the fractured-surface micrograph (toughening mechanism B) [37,38]. Micro cavities are seen surrounding nanoparticles due to weak interaction between the nanoparticle and polymer matrix (Figure 8c). The formation of voids actually leads to toughening of the system due to crack resistance and deflection; however, it cannot be said that plastic void growth contributes as a major toughening mechanism because we observed other toughening mechanisms as well. The governing mechanism can only be understood by the extent of dispersion of nanoparticles inside the matrix. Good dispersion generally results in higher strength since the crack can propagate through the matrix and either above or the below the poles of the strongly bonded nanofiller (toughening mechanism D) [35]. Increasing the nanoparticle concentration will result in aggregations that would generate areas with high stress concentration and make the stress/strain distribution through the matrix non-uniform. This region is susceptible to rapid and unstable crack propagation which leads to early mechanical failure of the system. Dispersion of nano fillers inside the polymer matrix is crucial and should be kept optimal for its superior performance.

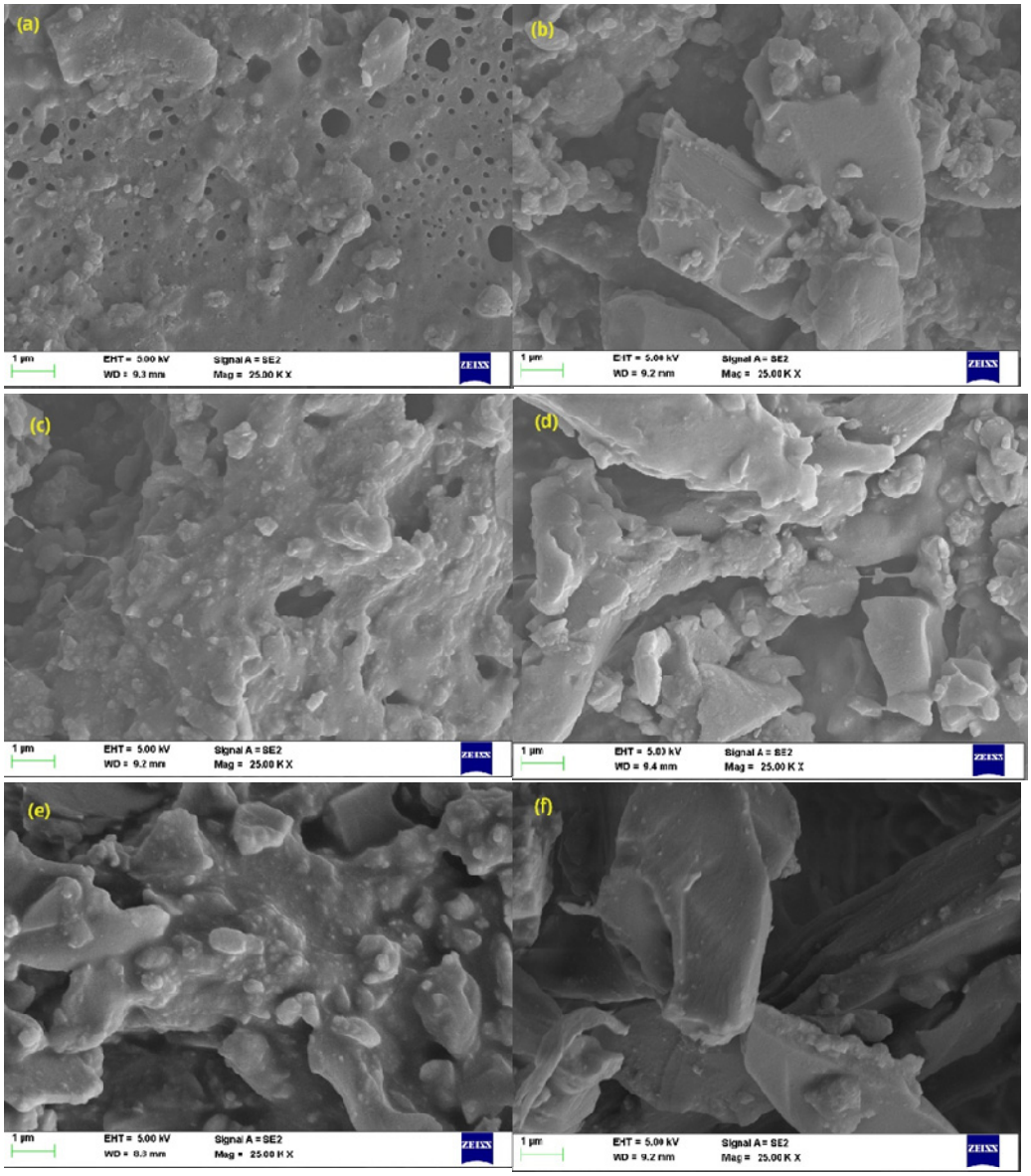

Figure 8. Tensile fractured SEM micrographs of (a) pure epoxy, (b) epoxy/0.5wt% ZTA, (c) epoxy/1.0wt% ZTA, (d) epoxy/1.5wt% ZTA, (e) epoxy/2.0wt% ZTA and (f) epoxy/2.5wt% ZTA.

3.9. Electrical properties

Breakdown voltage and break down strength of nano ZTA/epoxy composites were found to increase with increase in filler concentration as shown in Figure 9 The lowest breakdown voltage was observed for plain epoxy (13.54 kV) whereas the highest breakdown voltage was observed for epoxy loaded with 2.5 wt% ZTA nanoparticles (47.02 kV). Steep increase in breakdown voltage of 43.19 kV was observed for epoxy with 0.5 wt% ZTA, which is 218.98% higher as compared to plain epoxy as indicated in Table 5. This drastic increase in breakdown voltage is contributed by many factors such as uniform distribution of nano sized ZTA molecules in epoxy matrix, enhanced interfacial phenomena occurring between the matrix and filler component due to increase in surface

area of the ZTA nanoparticles and increase in the volume of epoxy surrounding the ZTA nanoparticles leading to a phenomenon called as high interaction zone [39]. The high interaction zone plays a vital role as it contributes to a remarkable increase in the breakdown strength at high voltage for all the epoxy-ZTA composites. When the epoxy is loaded with a nanofiller, the nanoparticle acts as a scattering site and does not allow the electron to gain momentum to induce breakdown. Only under the application of high electric field, the electrons get ejected and accelerated. These ejected electrons further collide with the uniformly distributed nanoparticles in epoxy, resulting in the loss of momentum. Only under the application of high voltage, the insulating material can be damaged or a catastrophic failure could occur. Thus, the aforementioned reasons contribute to profound increase in the breakdown voltage of epoxy-ZTA composites making it an advanced ceramic material suitable for high voltage insulation applications.

The breakdown voltage values obtained for our present work was compared with the literature values obtained by other researchers are as shown in Table 6. It is clearly evident that, 2.5 wt% ZTA in epoxy composite exhibited much higher breakdown down voltage compared to alumina/epoxy composites (56.73%) [39] and zirconia/epoxy composites (213.46%) [14] respectively. This kind of a drastic increase in breakdown voltage for epoxy-ZTA composites as compared to other composites has been contributed due to reason that, ZTA is a mixed metal oxide, in its nano form exhibiting excellent structural properties, has high resistance to catastrophic failure in stress induced environments and is a highly advanced ceramic material compared to nano alumina and nano zirconia [10]. These properties make epoxy-ZTA composites most desirable material for high voltage insulation applications.

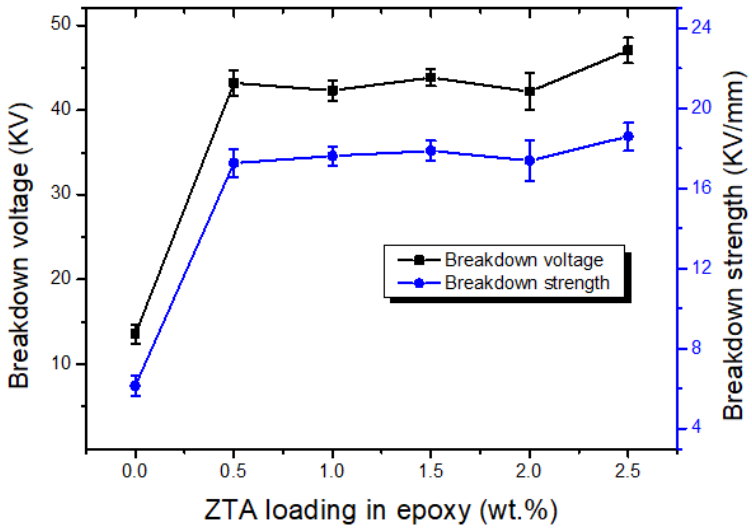

Figure 9. Breakdown voltage and breakdown strength of plain epoxy and nano ZTA/epoxy composites.

Table 5. Electrical properties of plain epoxy and nano ZTA/epoxy composites.

ZTA content (wt%)	Breakdown voltage (KV)	Increase in breakdown voltage (%)	Breakdown strength (KV/mm)	Increase in breakdown strength (%)
0.0*	13.54	-	6.15	-
0.5	43.19	218.98	17.27	180.91
1.0	42.30	212.40	17.62	186.85
1.5	43.84	223.78	17.89	190.89
2.0	42.20	211.66	17.40	182.92
2.5	47.02	247.26	18.60	202.43

*refers to plain epoxy.

Table 6. Comparative case study of breakdown voltage values for present work with literature values.

Composite synthesized	Highest Break down Voltage achieved (KV)	% higher compared to literature values	Literatures
Epoxy-Al_2O_3 (5 wt%)	30	56.73	[39]
Epoxy-ZrO_2 (2 wt%)	15	213.46	[14]
Epoxy-ZTA (2.5 wt%)	47.02	-	Chaitra et al. (Our present work)

4. Conclusion

ZTA nanoparticles were synthesized by solution combustion method. The nanoparticles were further characterised for their morphology and their structural properties using SEM, XRD and FTIR spectra. The results showed that XRD results revealed that zirconia existed in tetragonal phase and alumina existed hexagonal phase. Crystal size was analysed using Debye-Scherrer formula and average particle size of ZTA nanopowder was found to be around 30–50 nm. Doping ZTA into epoxy matrix showed an interesting transformation of the polymer from semi-crystalline to crystalline nature. SEM results showed that, ZTA nanoparticles were distributed homogenously and spherical in shape. TGA and DTG results showed enhanced stability of epoxy composites at higher temperatures. ZTA nanoparticles were doped into epoxy and the mechanical properties such as tensile properties, compressive properties and flexural properties were analysed. Enhanced Young's modulus values were observed. A common phenomenon was observed for both compressive properties as well as flexural properties of the ZTA filled epoxy composites. Highest values of compressive properties and flexural properties were observed for 1.5 wt% ZTA in epoxy, further addition of ZTA nanoparticles led to a drastic fall of both compressive properties as well as flexural properties. This phenomenon might have aroused due to the better adherence, good interfacial interactions and better load bearing capacity between epoxy and ZTA nanoparticles at 1.5 wt% concentration. These results suggest that, epoxy with 1.5 wt% loading of ZTA nanoparticles are well suited for mechanical applications. Breakdown voltage of epoxy-ZTA composites exhibited superior breakdown voltage performance as compared to plain epoxy. Epoxy loaded with 2.5 wt% ZTA nanoparticles showed highest breakdown voltage value of 47.02 kV due to formation of high interaction zone between epoxy and ZTA nanoparticles indicating that epoxy-ZTA composites are well suited for high voltage insulation applications that have high resistance to catastrophic failure in stress induced environments such as electrical circuits and transformer windings.

Acknowledgements

The authors are very grateful to Department of Science and Technology, for providing financial assistance under Women Scientist Scheme-A to carry out the entire project. Project Sanction No. SR/WOS-A/ET-16/2017. They are also thankful to Department of Chemical Engineering, MSRIT, Bangalore, for the technical support and Centre for Advanced Materials Technology of MSRIT, Bangalore for providing facility for research work. The authors are thankful to Dr. Pradeep Kumar Dixit, Department of Electrical and Electronics Engineering MSRIT, Bangalore for performing breakdown voltage test at their facility. Mechanical testing was performed at TERI, Bangalore.

Conflict of interest

The authors declare that they have no conflict of interest.

References

1. Wetzel B, Haupert F, Zhang MQ (2003) Epoxy nanocomposites with high mechanical and tribological performance. *Compos Sci Technol* 63: 2055–2067. https://doi.org/10.1016/S0266-3538(03)00115-5
2. Carolan D, Ivankovic A, Kinloch AJ, et al. (2017) Toughened carbon fibre-reinforced polymer composites with nanoparticle-modified epoxy matrices. *J Mater Sci* 52: 1767–1788. https://doi.org/10.1007/s10853-016-0468-5
3. Dorigato A, Pegoretti A, Bondioli F, et al. (2010) Improving epoxy adhesives with zirconia nanoparticles. *Compos Interface* 17: 873–892. https://doi.org/10.1163/092764410X539253
4. Bondioli F, Cannillo V, Fabbri E, et al. (2006) Preparation and characterization of epoxy resins filled with submicron spherical zirconia particles. *Polimery* 51: 794–798. https://doi.org/10.14314/polimery.2006.794
5. Dorigato A, Pegoretti A (2011) The role of alumina nanoparticles in epoxy adhesives. *J Nanopart Res* 13: 2429–2441. https://doi.org/10.1007/s11051-010-0130-0
6. Yu ZQ, You SL, Yang ZG, et al. (2011) Effect of surface functional modification of nano-alumina particles on thermal and mechanical properties of epoxy nanocomposites. *Adv Compos Mater* 20: 487–502. https://doi.org/10.1163/092430411X579104
7. Reyes-Rojas A, Dominguez-Rios C, Garcia-Reyes A, et al. (2018) Sintering of carbon nanotube-reinforced zirconia-toughened alumina composites prepared by uniaxial pressing and cold isostatic pressing. *Mater Res Express* 5: 105602. https://doi.org/10.1088/2053-1591/aada35
8. Chuankrerkkul N, Somton K, Wonglom T, et al. (2016) Physical and mechanical properties of zirconia toughened alumina (ZTA) composites fabricated by powder injection moulding. *Chiang Mai J Sci* 43: 375–380.
9. Ponnilavan V, Kannan S (2019) Structural, optical tuning, and mechanical behavior of zirconia toughened alumina through europium substitutions. *J Biomed Mater Res Part B* 107: 1170–1179. https://doi.org/10.1002/jbm.b.34210
10. Srikanth C, Madhu GM (2020) Effect of ZTA concentration on structural, thermal, mechanical and dielectric behavior of novel ZTA-PVA nanocomposite films. *SN Appl Sci* 2: 1–12. https://doi.org/10.1007/s42452-020-2232-3

11. Zhang J, Ge L, Chen ZG, et al. (2019) Cracking behavior and mechanism of gibbsite crystallites during calcination. *Cryst Res Technol* 54: 1800201. https://doi.org/10.1002/crat.201800201
12. Bhaduri S, Bhaduri SB, Zhou E (1998) Auto ignition synthesis and consolidation of Al_2O_3–ZrO_2 nano/nano composite powders. *J Mater Res* 13: 156–165. https://doi.org/10.1557/JMR.1998.0021
13. Vasylkiv O, Sakka Y, Skorokhod VV (2003) Low-temperature processing and mechanical properties of zirconia and zirconia–alumina nanoceramics. *J Am Ceram Soc* 86: 299–304. https://doi.org/10.1111/j.1151-2916.2003.tb00015.x
14. Sagar JS, Kashyap SJ, Madhu GM, et al. (2020) Investigation of mechanical, thermal and electrical parameters of gel combustion-derived cubic zirconia/epoxy resin composites for high-voltage insulation. *Cerâmica* 66: 186–196. https://doi.org/10.1590/0366-69132020663782887
15. Ho MW, Lam CK, Lau K, et al. (2006) Mechanical properties of epoxy-based composites using nanoclays. *Compos Struct* 75: 415–421. https://doi.org/10.1016/j.compstruct.2006.04.051
16. Uhl FM, Davuluri SP, Wong SC, et al. (2004) Organically modified montmorillonites in UV curable urethane acrylate films. *Polymer* 45: 6175–6187. https://doi.org/10.1016/j.polymer.2004.07.001
17. Nguyen TA, Nguyen TV, Thai H, et al. (2016) Effect of nanoparticles on the thermal and mechanical properties of epoxy coatings. *J Nanosci Nanotechnol* 16: 9874–9881. https://doi.org/10.1166/jnn.2016.12162
18. Baiquni M, Soegijono B, Hakim AN (2019) Thermal and mechanical properties of hybrid organoclay/rockwool fiber reinforced epoxy composites. *J Phys Conf Ser* 1191: 012056. https://doi.org/10.1088/1742-6596/1191/1/012056
19. Zhang X, Alloul O, He Q, et al. (2013) Strengthened magnetic epoxy nanocomposites with protruding nanoparticles on the graphene nanosheets. *Polymer* 54: 3594–3604. https://doi.org/10.1016/j.polymer.2013.04.062
20. Nazarenko OB, Melnikova TV, Visakh PM (2016) Thermal and mechanical characteristics of polymer composites based on epoxy resin, aluminium nanopowders and boric acid. *J Phys Conf Ser* 671: 012040. https://doi.org/10.1088/1742-6596/671/1/012040
21. Sand Chee S, Jawaid M (2019) The effect of Bi-functionalized MMT on morphology, thermal stability, dynamic mechanical, and tensile properties of epoxy/organoclay nanocomposites. *Polymers* 11: 2012. https://doi.org/10.3390/polym11122012
22. Bikiaris D (2011) Can nanoparticles really enhance thermal stability of polymers? Part II: An overview on thermal decomposition of polycondensation polymers. *Thermochim Acta* 523: 25–45. https://doi.org/10.1016/j.tca.2011.06.012
23. Xue Y, Shen M, Zeng S, et al. (2019) A novel strategy for enhancing the flame resistance, dynamic mechanical and the thermal degradation properties of epoxy nanocomposites. *Mater Res Express* 6: 125003. https://doi.org/10.1088/2053-1591/ab537f
24. Colomban P (1989) Structure of oxide gels and glasses by infrared and Raman scattering. *J Mater Sci* 24: 3011–3020. https://doi.org/10.1007/BF02385660
25. Taavoni-Gilan A, Taheri-Nassaj E, Naghizadeh R, et al. (2010) Properties of sol-gel derived Al_2O_3–15 wt% ZrO_2 (3 mol% Y_2O_3) nanopowders using two different precursors. *Ceram Int* 36: 1147-1153. https://doi.org/10.1016/j.ceramint.2009.11.011
26. Noma T, Sawaoka A (1984) Fracture toughness of high pressure sintered Al_2O_3–ZrO_2 ceramics. *J Mater Sci Lett* 3: 533–535. https://doi.org/10.1007/BF00720992

27. Shukla DK, Kasisomayajula SV, Parameswaran V (2008) Epoxy composites using functionalized alumina platelets as reinforcements. *Compos Sci Technol* 68: 3055–3063. https://doi.org/10.1016/j.compscitech.2008.06.025
28. Abbate M, Martuscelli E, Musto P, et al. (1994) Toughening of a highly cross-linked epoxy resin by reactive blending with bisphenol A polycarbonate. I. FTIR spectroscopy. *J Polym Sci Pol Phys* 32: 395–408. https://doi.org/10.1002/polb.1994.090320301
29. Katon JE, Bentley FF (1963) New spectra-structure correlations of ketones in the 700–750 cm^{-1} region. *Spectrochim Acta* 19: 639–653. https://doi.org/10.1016/0371-1951(63)80127-7
30. Magnani G, Brillante A (2005) Effect of the composition and sintering process on mechanical properties and residual stresses in zirconia–alumina composites. *J Eur Ceram Soc* 25: 3383–3392. https://doi.org/10.1016/j.jeurceramsoc.2004.09.025
31. Ashamol A, Priyambika VS, Avadhani GS, et al. (2013) Nanocomposites of crosslinked starch phthalate and silane modified nanoclay: Study of mechanical, thermal, morphological, and biodegradable characteristics. *Starch-Stärke* 65: 443–452. https://doi.org/10.1002/star.201200145
32. Jumahat A, Soutis C, Mahmud J, et al. (2012) Compressive properties of nanoclay/epoxy nanocomposites. *Procedia Eng* 41: 1607–1613. https://doi.org/10.1016/j.proeng.2012.07.361
33. Abbass A, Abid S, Özakça M (2019) Experimental investigation on the effect of steel fibers on the flexural behavior and ductility of high-strength concrete hollow beams. *Adv Civ Eng* 2019: 8390345. https://doi.org/10.1155/2019/8390345
34. Konnola R, Deeraj BDS, Sampath S, et al. (2019) Fabrication and characterization of toughened nanocomposites based on TiO_2 nanowire-epoxy system. *Polym Compos* 40: 2629–2638. https://doi.org/10.1002/pc.25058
35. Zhao S, Schadler LS, Duncan R, et al. (2008) Mechanisms leading to improved mechanical performance in nanoscale alumina filled epoxy. *Compos Sci Technol* 68: 2965–2975. https://doi.org/10.1016/j.compscitech.2008.01.009
36. Goyat MS, Rana S, Halder S, et al. (2018) Facile fabrication of epoxy-TiO_2 nanocomposites: a critical analysis of TiO_2 impact on mechanical properties and toughening mechanisms. *Ultrason Sonochem* 40: 861–873. https://doi.org/10.1016/j.ultsonch.2017.07.040
37. Johnsen BB, Kinloch AJ, Mohammed RD, et al. (2007) Toughening mechanisms of nanoparticle-modified epoxy polymers. *Polymer* 48: 530–541. https://doi.org/10.1016/j.polymer.2006.11.038
38. Johnsen BB, Kinloch AJ, Taylor AC (2005) Toughness of syndiotactic polystyrene/epoxy polymer blends: microstructure and toughening mechanisms. *Polymer* 46: 7352–7369. https://doi.org/10.1016/j.polymer.2005.05.151
39. Mohanty A, Srivastava VK (2013) Dielectric breakdown performance of alumina/epoxy resin nanocomposites under high voltage application. *Mater Design* 47: 711–716. https://doi.org/10.1016/j.matdes.2012.12.052